

Conversion of bound excitons to free excitons by surface acoustic waves

S. Völkl,^{1,2} A. Wixforth,^{1,2} D. Reuter,³ A. D. Wieck,³ and J. Ebbecke^{1,2,4}

¹*Institut für Physik der Universität Augsburg, Experimentalphysik I, Universitätsstr. 1, 86159 Augsburg, Germany*

²*Center for NanoScience (CeNS), Geschwister-Scholl-Platz 1, 80539 Munich, Germany*

³*Angewandte Festkörperphysik, Ruhr-Universität Bochum, 44780 Bochum, Germany*

⁴*NanoSYD, Mads Clausen Institute, University of Southern Denmark, Alsion 2, DK 6400 Sonderborg, Denmark*

(Received 13 August 2009; published 6 October 2009)

We present detailed investigations of the surface acoustic wave-mediated dissociation of bound and free excitons in a GaAs multi-quantum well. The energetic position of the photoluminescence spectrum can be assigned to the single quantum wells of different width and distance from the sample surface. The effect of the piezoelectric field on the efficiency of excitation dissociation in the different quantum wells is characterized. For certain experimental conditions bound excitons are converted to free excitons by the surface acoustic wave and possible explanations are described.

DOI: [10.1103/PhysRevB.80.165307](https://doi.org/10.1103/PhysRevB.80.165307)

PACS number(s): 78.20.Hp, 78.67.De, 78.55.Cr

I. INTRODUCTION

Surface acoustic waves (SAWs) are mechanical waves propagating along the surface of a substrate.¹ On piezoelectric materials electric fields accompany these mechanical waves. III-V semiconductors are piezoelectric and exhibit excitonic light emission at the same time. Therefore these materials are ideal systems for studying the interaction between SAW-induced piezoelectric fields and the photoluminescence (PL) behavior. In quantum-well (QW) structures based on III-V compounds excitons are confined vertically. As the piezoelectric field of a SAW consists of a lateral and a vertical part, the lateral component can dissociate this excitonic state,² whereas the vertical component only shifts the emission wavelength.³ Thus a SAW propagating along a QW structure quenches the PL peak due to the lateral component.^{4,5}

Depending on the studied system excitons can be trapped locally, for example, by impurities or interface defects.^{6–10} Trapped or bound excitons (BXs) bind to their binding centers and differ from free excitons (FXs) in an extra binding energy. An additional peak in the PL spectra reveals their existence. Recombination of excitons is possible via the FX and the BX channels. We present detailed investigations of the SAW-mediated effect of exciton dissociation in GaAs QWs. In order to study the influence of different quantum-well widths on the PL at the same time, a GaAs/AlAs multi-quantum-well (MQW) structure was chosen. Unexpectedly, we found that the SAW can convert bound excitons into free excitons at certain experimental conditions.

II. RESULTS AND DISCUSSION

A. Sample

Starting with the substrate material GaAs, 11 GaAs QWs with different widths were grown by molecular-beam epitaxy. The barriers between the QWs are 23.8 nm thick short period superlattices composed of five times 2.6 nm AlAs, separated by four times 2.7 nm GaAs layers. The emission wavelength of the PL signal depends on the QW width. Therefore the PL peaks can be assigned to the corresponding

QWs, respectively, sample depths. Table I gives an overview of these parameters. In spite of the complexity of the MQW heterostructure it was preferred to several samples with individual QWs. A single sample guarantees to have the same SAW propagating along all QWs. The field profile of the SAW varies with sample depth but can be calculated (see Sec. II G).

Using *e*-beam lithography two pairs of interdigital transducers (IDTs) forming perpendicular delay lines have been processed in order to probe two different time scales. The periodicities of the transducers are $\lambda_1=8\ \mu\text{m}$ and $\lambda_2=4\ \mu\text{m}$. A SAW can be launched by supplying the IDTs with a voltage signal at their resonance frequencies. For the two delay lines these resonance frequencies are $f_1=367\ \text{MHz}$ and $f_2=745\ \text{MHz}$, respectively. The sound paths of the two delay lines are $300\ \mu\text{m}$ wide and cross the middle of the sample where the laser spot for all PL measurements was adjusted to. The higher SAW frequency is in the regime of exciton life times ($\tau\approx 1\ \text{ns}$). Therefore the PL dependence on SAW power should differ significantly for the two frequencies.

B. Experimental setup

For obtaining PL spectra a micro-PL setup is used. The sample is mounted inside a flow cryostat operated with liquid

TABLE I. Overview of sample structure and emission wavelengths. Units are in nm.

Sample depth	QW width	Emission wavelength
97.2	4.5	763
125.8	5.1	772
154.8	5.3	782
185.4	8.3	792
218.3	9.9	801
253.1	12.2	807
290.6	15.2	812
331.9	19.8	818

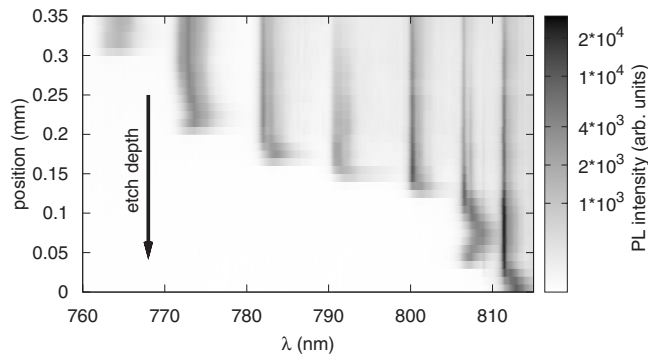


FIG. 1. Spatial dependence of PL emission of wedge-shaped etched MQW structure. Peaks disappear successively for increasing etch depth. Temperature was 4.2 K.

helium and is situated right below a quartz window. The cryostat is equipped with four coax lines for supply of the IDTs and a xyz stage for positioning the sample. A diode laser excites the sample through the window at a wavelength of 675 nm with a maximal optical power of 5 mW. Both the exciting laser light and the emitted PL light pass through the same $50\times$ microscope objective. The size of the focused laser spot on the sample surface is about $5\ \mu\text{m}$ in diameter. A spectrometer analyses the PL light where mostly a grating with 1800 gr/mm is used. The charge coupled device detector of the spectrometer is cooled with liquid nitrogen for a high signal-to-noise ratio.

C. PL emission wavelengths and corresponding QWs

To assign the different QWs to their PL signals (see Table I) the quantized states of the QWs and out of it the expected emission energies can be calculated. Such calculations were done via the simulation software 1D POISSON solver.¹¹

By etching the sample surface to a wedge shape and measuring the PL along the etch gradient an experimental assignment is also possible. Due to the special arrangement of QWs in the studied structure—thinner QWs lie closer to the surface than wider QWs—each PL peak can be assigned to its corresponding QW in sequential order. For this purpose a piece of the sample material was covered on one half with photoresist and then slowly pulled out of a wet etchant. The etch depth was checked using a height profiler to ensure that the whole range was obtained from unetched sample surface up to a depth where all QWs were removed. The PL measurements along the wedge are shown in Fig. 1. The PL peaks disappear successively when the position of the laser focus on the sample surface is moved toward increasing etch depths. The peak shapes change when the QWs are getting very close to the etched surface.

Taking both methods into account it was possible to assign eight PL peaks to their corresponding QW. Therefore only these peaks (see Table I) will be considered.

D. SAW experiment

A more detailed analysis of the PL spectra exhibits that each PL signal is not a single peak but consists of a main

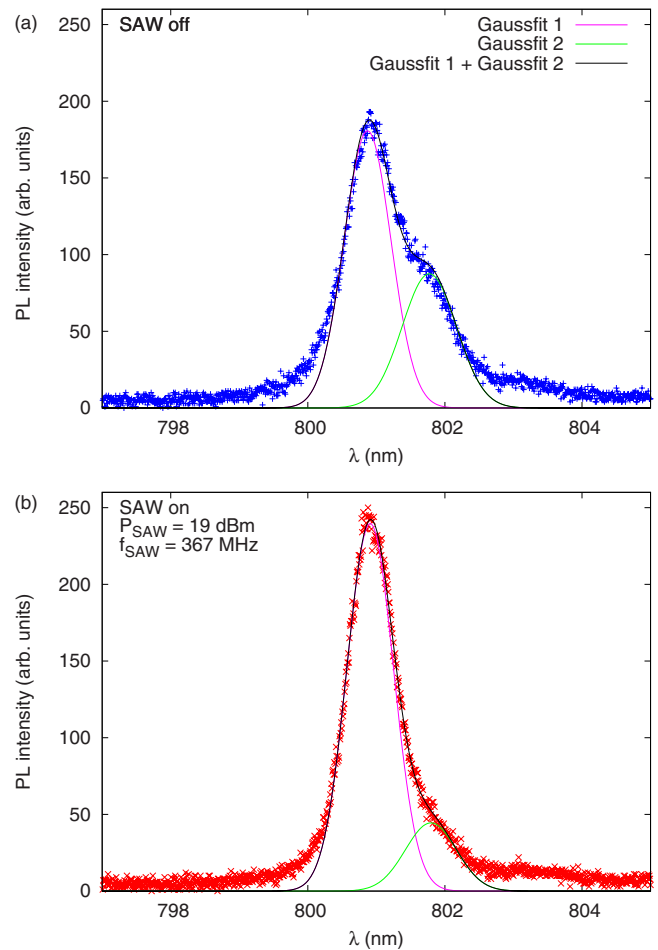


FIG. 2. (Color online) Two PL spectra of the 9.9 nm wide QW: (a) without SAW excitation and (b) with SAW excitation. Laser intensity was 380 nW and temperature 6 K. The experimental data is also fitted using Gaussian curves.

peak at the short wave side and one with smaller intensity apparent as a shoulder on the long wave side. Figure 2(a) reveals that for the 801 nm PL signal. Both parts are fitted using Gaussian curves. In Fig. 2(b) additionally a SAW was launched using one of the IDTs with lower periodicity λ_1 .

When the SAW is applied the short wave part of the double peak is increased whereas the long wave part shrinks. For the given SAW power level of 19 dBm the integrated total PL intensity remains almost constant. As proven in the etch experiment both parts must originate from the same QW because both parts vanish simultaneously.

The result of this experiment contradicts earlier investigations^{4,5,12} where the lateral piezoelectric SAW field was used to dissociate excitons. In those experiments always a decrease in the excitonic transition was observed. This behavior is well described in literature as PL quenching.

E. Proposed model

To explain the surprising behavior of the PL peak redistribution by applying a SAW the following model is proposed: The left main peak of the PL signals belongs to free excitons whereas the right peak belongs to bound excitons.

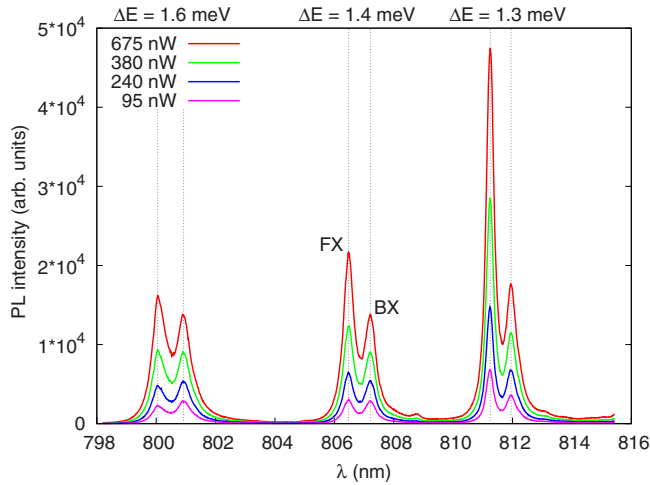


FIG. 3. (Color online) Excitation intensity series for three adjacent QWs. The excitation intensity was varied by attenuating the laser beam by neutral density filters. Temperature was 4.2 K. Above the splitting energies between the FX and BX peaks are calculated.

Bound excitons differ from free excitons in an additional binding to local defects. The piezoelectric SAW field breaks this binding and triggers a conversion of BX to FX which leads to a decrease in the BX signal whereas the FX signal increases.

F. Evidence of model

The nature of the BX peaks is ambiguous. Several types of binding mechanisms are considered. Impurities in terms of donors or acceptors may lead to a binding of excitons.⁶⁻⁹ However there are low impurity densities assumed for the studied sample material. Hence it is more likely that other binding centers like interface defects¹⁰ play an important role.

In Fig. 3 the PL of the 9.9-, 12.2-, and 15.2-nm-wide QW are shown. These measurements have been made on the unetched part of the wedged sample. The laser power was attenuated gradually by neutral density filters. By decreasing the excitation intensity the ratio between BX and FX emission shifts in favor of the BX peaks which is in agreement with Ref. 13. Leaving the laser power constant the BX/FX ratio decreases when the QW width is increased. That can be explained if the binding centers are situated mainly at the interfaces of the heterostructure. Then the surface-volume, respectively, BX/FX ratio should be higher for thinner QWs. The BX binding energy can be determined by measuring the spectral splitting of the BX peak to the FX peak. BX binding energies are in the order of 1.5 meV and depend strongly on the well width. The authors of Ref. 14 calculated this dependency. Our values shown in the upper part of Fig. 3 agree with the expected decrease in BX binding energy as the well width is increased.

The FX binding energy is about five times larger than the BX bond.^{14,15} In order to initiate a significant dissociation the excitons must be exposed to an energy which is of the same order as the respective binding energy. Hence, the thermal

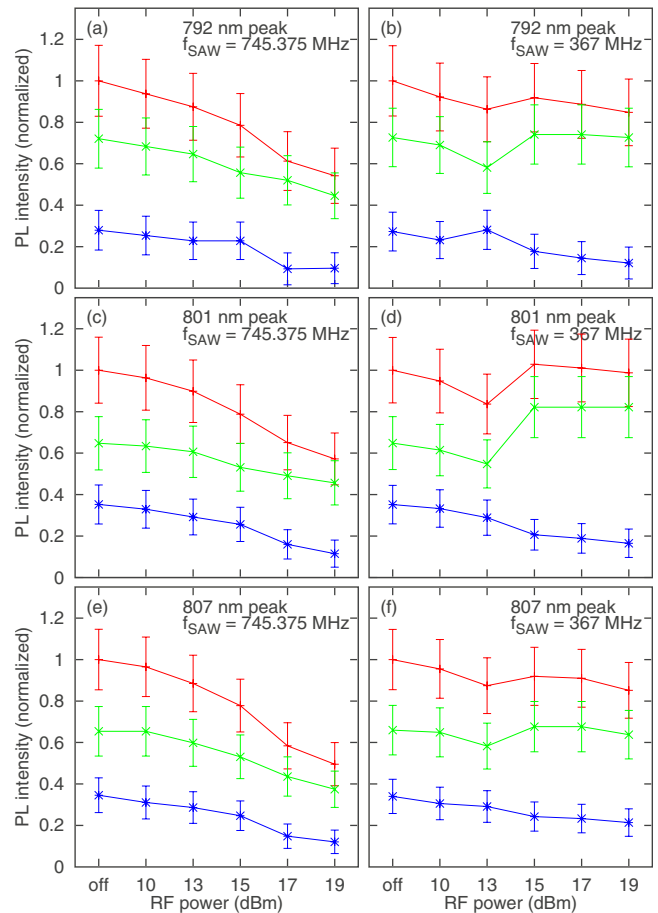


FIG. 4. (Color online) PL intensity as function of SAW power for three transitions corresponding to three different QW widths and two SAW frequencies. Red (top): total PL, green (middle): FX, and blue (bottom): BX. Each value was calculated by fitting and integrating the spectra using Gaussian functions. The FX and BX intensities are normalized to the total PL where no SAW was applied. All values were recorded at the same sample position. Temperature was 4.2 K.

energy $k_B T$ is one example of energy supply which can lead to “melting” of excitons.¹⁶⁻¹⁸

In Fig. 4 the integrated PL intensities of three adjacent QWs are shown as a function of SAW power. On the left-hand side the values for the high-frequency SAW and on the right-hand side the values for the lower frequency are presented. Each graph shows the integrated PL of the FX transition, the BX transition, and their sum. For the higher frequency SAW all PL intensities decrease monotonically with increasing SAW power. Only for the lower frequency SAW an enhancement of the FX peaks occurs. The FX enhancement starts for all three QWs at a threshold power level of 15 dBm and coincides with a distinct decrease in the bound exciton PL signal. According to Refs. 19-22 the occurrence of a sharp threshold indicates an impact ionization process.

Santos *et al.*¹² investigated the impact ionization of bound excitons in bulk GaAs by piezoelectric SAW fields. The model they presented based on the reduction in the effective exciton binding energy in the presence of an electric field,

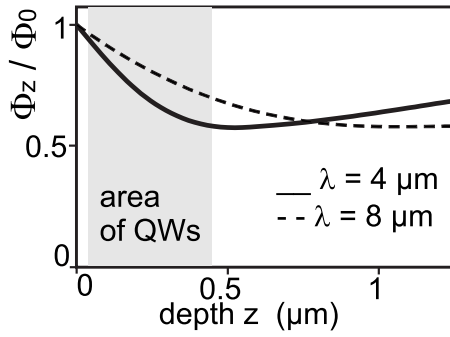


FIG. 5. The normalized piezoelectric SAW potential along the vertical direction for two SAW wavelengths (Ref. 26). QWs lie within the gray highlighted area.

$$E_{ex} = E_{ex}(0) - E_k \quad \text{with} \quad E_k \sim \frac{1}{2} m^* (\mu \mathcal{E})^2. \quad (1)$$

Out of it they calculated PL quenching rates. In contrast to our results no PL enhancement was observed. Also, the effect of a SAW on the dissociation of free and bound excitons has been investigated by other groups in materials such as bulk GaAs (Ref. 23) and GaN heterostructures^{24,25} but here we report for the first time the SAW-mediated conversion of bound excitons to free excitons in GaAs QWs. As already highlighted in Fig. 2 and presented in more detail in Fig. 4 the decrease in light emission from the BX transition at a SAW power of 15 dBm coincides with the PL enhancement of the FX signal. That leads us to the conclusion that the SAW breaks the bond of the bound exciton to its binding center (such as interface defect) and therefore converts the BX into a FX which subsequently recombines.

G. SAW depth profile

The MQW layers span a sample depth ranging from 40 to 445 nm. Thus the QW closest to the surface is exposed to another piezoelectric SAW potential than the very last one. Therefore great importance must be attached to the depth dependency of this potential. The piezoelectric potential of a SAW (Rayleigh type) can be calculated by a Laguerre polynomial approach.²⁶ The authors of Ref. 27 extended this approach to III-V semiconductor quantum-well structures. The overall piezoelectric potential is given by

$$\Phi(\vec{r}, t) = \Phi(z) \exp[i(\omega t - kx)]. \quad (2)$$

In the case of QWs mainly the lateral field component E_x is assumed to contribute to the impact ionization process of bound excitons. In vertical direction excitons are confined. Once the curve of the piezoelectric potential $\Phi(z)$ along the vertical direction is found, the electric field components E_z normal to the surface and E_x in direction of SAW propagation can be determined.^{27,28} With $E_x = -\frac{\partial \Phi(\vec{r}, t)}{\partial x}$ the lateral field component follows in z the well-known $\Phi(z)$ characteristic.²⁶⁻²⁸ Thus E_x and $\Phi(z)$ depict the same sample depth function that never becomes zero in the order of a SAW wavelength for fixed x and t . Therefore dissociation of bound excitons is expected to occur everywhere provided

that the field strengths are high enough for the impact ionization process.

Figure 5 shows the piezoelectric SAW potential for both SAW periods. All QWs of the heterostructure lie within the highlighted region.

The outermost QW perceives the highest potential, respectively, lateral field component and the innermost QW a weaker one. Across the relevant region this difference is never larger than 40%. Therefore the PL quenching, respectively, enhancement effect is expected to be comparable for all QWs. In particular, the SAW depth profiles of the two SAW frequencies cannot account for the distinct PL behavior. Additionally, according to the potential profile shown in Fig. 5, the strength of the z component of the SAW potential with higher frequency is always smaller in the area of the QWs compared to the lower frequency one. Therefore, a more pronounced effect of the higher frequency SAW could be expected. The reason why the excitonic conversion only occurs for the lower SAW frequency remains still under investigation. The difference of the temporal SAW period for the two frequencies in comparison to the exciton lifetimes may also play here a significant role. Time-resolved experiments can answer this question.²⁹

H. QW width

Due to different widths and distances to the surface the generation of charge carriers inside the QWs and the emission of PL light should occur with different efficiencies. Furthermore charge carriers of one QW layer could screen the piezoelectric SAW field inside another one. In order to balance the differences between the QWs the incident laser intensity can be adjusted for each QW. In order to exclude screening effects the laser intensity was kept low ($< 5 \mu\text{W}$). That reduces the total amount of charge carriers.

The binding energy E_{BX} of a bound exciton to its binding center has a dependence on the QW width L_z with a maximum in binding energy at approximately 10 nm.⁹ Hence the SAW fields required to dissociate the BX bond depend on L_z too. However Weman *et al.*²² consider this dependence to be too weak to explain the threshold fields for QWs thinner than 10 nm. They assumed the charge-carrier mobility to play an important role. The mobility decreases with decreasing well width due to scattering at the interfaces.³⁰ If the mobility of the charge carriers decreases, higher electric field strengths are required to reach kinetic energies in the order of E_{BX} . Furthermore the bound exciton lifetime τ_{BX} and the QW width L_z are related to each other. After Ref. 31 the lifetime is indirect proportional to the binding energy which depends on L_z .¹⁴ Therefore excitons decay faster in thinner QWs than in wider ones. As the decay rates become higher, less time remains for the dissociation process by piezoelectric fields. That could explain the less pronounced PL quenching and FX enhancement which was observed for the thinner QWs of the MQW structure (not shown) and the measured maximal conversion of BX to FX in case of the QW with 9.9 nm thickness.

III. CONCLUSION

In summary, we demonstrated the conversion of bound excitons to free excitons in GaAs QWs by surface acoustic

waves. The proposed model of this conversion process was supported experimentally by an excitation intensity series and a SAW power series where two SAW frequencies were used. In bulk GaAs and GaN heterostructures similar conversion processes were already reported and explained by impact ionization. These results agree qualitatively with ours which suggests impact ionization also for the BX bond of the investigated MQW structure. Furthermore the effect of the piezoelectric SAW depth profile was studied. It turns out not to be the explanation for a different PL behavior of different QWs inside the heterostructure. Rather QW-dependent pa-

rameters such as charge-carrier mobility and exciton lifetimes determine these differences.

ACKNOWLEDGMENTS

The authors would like to thank F. Haake, S. W. Koch, M. Mack, and W. Hoyer for helpful discussions and G. Snider for providing the 1D POISSON solver. D.R. and A.D.W. thank the DFG-GRK384 and the BMBF NanoQUIT for financial support. This work was supported in part by the German Government through the Cluster of Excellence NIM.

-
- ¹L. J. W. S. Rayleigh, Proc. London Math. Soc. **s1-17**, 4 (1885).
²D. A. B. Miller, D. S. Chemla, T. C. Damen, A. C. Gossard, W. Wiegmann, T. H. Wood, and C. A. Burrus, Phys. Rev. B **32**, 1043 (1985).
³D. A. B. Miller, D. S. Chemla, T. C. Damen, A. C. Gossard, W. Wiegmann, T. H. Wood, and C. A. Burrus, Phys. Rev. Lett. **53**, 2173 (1984).
⁴C. Roche, S. Zimmermann, A. Wixforth, J. P. Kotthaus, G. Böhm, and G. Weimann, Phys. Rev. Lett. **78**, 4099 (1997).
⁵C. Roche, A. O. Govorov, A. Wixforth, G. Böhm, and G. Weimann, Phys. Rev. B **57**, R6850 (1998).
⁶E. H. Bogardus and H. B. Bebb, Phys. Rev. **176**, 993 (1968).
⁷D. Bimberg, H. Münzel, A. Steckenborn, and J. Christen, Phys. Rev. B **31**, 7788 (1985).
⁸R. C. Miller, A. C. Gossard, W. T. Tsang, and O. Munteanu, Phys. Rev. B **25**, 3871 (1982).
⁹D. C. Reynolds, C. E. Leak, K. K. Bajaj, C. E. Stutz, R. L. Jones, K. R. Evans, P. W. Yu, and W. M. Theis, Phys. Rev. B **40**, 6210 (1989).
¹⁰G. Bastard, C. Delalande, M. H. Meynadier, P. M. Frijlink, and M. Voos, Phys. Rev. B **29**, 7042 (1984).
¹¹G. Snider (2007), 1D POISSON solver, www.nd.edu/~gsnider/
¹²P. V. Santos, M. Ramsteiner, and F. Jungnickel, Appl. Phys. Lett. **72**, 2099 (1998).
¹³S. Charbonneau, T. Steiner, M. L. W. Thewalt, E. S. Koteles, J. Y. Chi, and B. Elman, Phys. Rev. B **38**, 3583 (1988).
¹⁴D. A. Kleinman, Phys. Rev. B **28**, 871 (1983).
¹⁵R. L. Greene, K. K. Bajaj, and D. E. Phelps, Phys. Rev. B **29**, 1807 (1984).
¹⁶D. Bimberg, M. Sondergeld, and E. Grobe, Phys. Rev. B **4**, 3451 (1971).
¹⁷C. Delalande, M. H. Meynadier, and M. Voos, Phys. Rev. B **31**, 2497 (1985).
¹⁸S. Datta, B. M. Arora, and S. Kumar, Phys. Rev. B **62**, 13604 (2000).
¹⁹D. L. Smith, D. S. Pan, and T. C. McGill, Phys. Rev. B **12**, 4360 (1975).
²⁰W. Bludau and E. Wagner, Phys. Rev. B **13**, 5410 (1976).
²¹H. Weman, G. M. Treacy, H. P. Hjalmarson, K. K. Law, J. P. Bergman, J. L. Merz, and A. C. Gossard, Semicond. Sci. Technol. **7**, B517 (1992).
²²H. Weman, G. M. Treacy, H. P. Hjalmarson, K. K. Law, J. L. Merz, and A. C. Gossard, Phys. Rev. B **45**, 6263 (1992).
²³K. S. Zhuravlev, D. V. Petrov, Y. B. Bolkhovityanov, and N. S. Rudaja, Appl. Phys. Lett. **70**, 3389 (1997).
²⁴D. Nelson, B. Gil, M. A. Jacobson, V. D. Kagan, N. Grandjean, B. Beaumont, J. Massies, and P. Gibart, J. Phys.: Condens. Matter **13**, 7043 (2001).
²⁵J. Pedrós, Y. Takagaki, T. Ive, M. Ramsteiner, O. Brandt, U. Jahn, K. H. Ploog, and F. Calle, Phys. Rev. B **75**, 115305 (2007).
²⁶S. Datta and B. J. Hunsinger, J. Appl. Phys. **49**, 475 (1978).
²⁷C. Thompson and B. L. Weiss, J. Appl. Phys. **78**, 5002 (1995).
²⁸J. E. Lefebvre, V. Zhang, J. Gazalet, and T. Gryba, J. Appl. Phys. **83**, 28 (1998).
²⁹T. Sogawa, H. Sanada, H. Gotoh, H. Yamaguchi, S. Miyashita, and P. V. Santos, Appl. Phys. Lett. **94**, 131912 (2009).
³⁰R. Gottinger, A. Gold, G. Abstreiter, G. Weimann, and W. Schlapp, Europhys. Lett. **6**, 183 (1988).
³¹J. Feldmann, G. Peter, E. O. Göbel, P. Dawson, K. Moore, C. Foxon, and R. J. Elliott, Phys. Rev. Lett. **59**, 2337 (1987).